Measurement of the branching ratio of the ^{6}He β-decay channel into the $\alpha + d$ continuum

R. Raabe, J. Büscher, J. Ponsaers, F. Aksouh, M. Huyse, O. Ivanov, S. R. Lesher,* I. Mukha,† D. Pauwels, M. Sawicka, D. Smirnov, I. Stefanescu, J. Van de Walle,‡ and P. Van Duppen
Instituut voor Kern- en Stralingsfysica, Katholieke Universiteit Leuven, B-3001 Leuven, Belgium

C. Angulo, J. Cabrera,§ and N. de Séréville‖
Centre de Recherches du Cyclotron, Université Catholique de Louvain, Chemin du Cyclotron 2, B-1348 Louvain-la Neuve, Belgium

I. Martel and A. M. Sánchez-Benítez
Departamento de Física Aplicada, Facultad de Ciencias Experimentales, Campus de El Carmen, Avenida de las Fuerzas Armadas, Universidad de Huelva, E-21071 Huelva, Spain

C. Aa. Diget¶
Department of Physics and Astronomy, University of Aarhus, Ny Munkegade, Building 1520, DK-8000 Aarhus C, Denmark
(Received 29 June 2007; revised manuscript received 6 September 2009; published 16 November 2009)

We measured the deuteron-emission branch of the β decay of the halo nucleus ^{6}He using the technique of implantation into a highly segmented silicon detector. The method, used here for the first time with a beam of ^{6}He ions, ensures precise normalization; the value obtained for the branching ratio is $\bar{B} = (1.65 \pm 0.10) \times 10^{-6}$ (6% error). The summed energy spectra of the emitted α and d particles has also been measured. The results allow us to compare calculations from various models, potentially setting strong constraints on the precision required for the description of the ^{6}He ground-state wave function.

DOI: 10.1103/PhysRevC.80.054307 PACS number(s): 23.40.Hc, 27.20.+n

I. INTRODUCTION

To date, most experimental investigations performed on halo nuclei [1] have involved the measurement of nuclear reactions. In such cases, knowledge of the halo structure relies on model-dependent reaction mechanisms. However, the theory describing β decay is well established, offering an alternative and reliable probe to study halo properties. In addition, at large distances β decay is sensitive to the details of the wave function.

Peculiarities in the β decay of halo nuclei were identified from measurements at the ISOLDE facility in CERN [2]. The decay of these systems is characterized by large available energies (Q values) and by low breakup thresholds in the daughter nuclei, so that the feeding to continuum states and the subsequent emission of nucleons or ions becomes possible. The decay of the ^{6}He nucleus mainly proceeds to the ground state of ^{6}Li ($Q = 3.508$ MeV), but the $\alpha + d$ channel is also energetically allowed ($Q = 2.033$ MeV). This is also referred to as the β-delayed deuteron-emission channel, a peculiar decay mode heretofore observed only in the halo nuclei ^{6}He and ^{11}Li [3]. The corresponding branching ratio and the spectrum of the emitted particles depend on the ^{6}He ground-state wave function and the $\alpha + d$ interaction potential.

The first observation of deuteron emission in the decay of ^{6}He was made at ISOLDE [4]. The authors measured a branching ratio of $(2.8 \pm 0.5) \times 10^{-6}$ for a deuteron energy threshold of 350 keV. After a new experiment, the value was corrected to $(7.6 \pm 0.6) \times 10^{-6}$ [5]. More recently, another measurement performed at the TRIUMF facility [6] obtained the result $(1.8 \pm 0.9) \times 10^{-6}$ (for the same deuteron energy threshold), which is lower than the values obtained at ISOLDE. The large overall uncertainty associated with the TRIUMF result is related to the determination of the detection efficiency (geometrical factors and electronic threshold). However, large statistics allowed a precise measurement of the form of the energy spectrum of the emitted α and d particles.

At the time of the first measurements, all theoretical calculations predicted a much larger value for the $\alpha + d$ branching ratio: about 10^{-4} for an R-matrix model [4], 2×10^{-4} for a two-body model [7], and (3–4) $\times 10^{-5}$ for a three-body model [8]. The disagreement with experimental results was afterward explained in terms of a cancellation between two parts of the Gamow-Teller matrix element, related to the "internal" and "external" regions of the ^{6}He ground state and the $\alpha + d$ scattering wave functions, respectively, and in terms of overlaps in the two regions that have similar magnitudes but opposite signs. This property was first detected in a semi-microscopic study [9], and then confirmed in successive works with an improved model for ^{6}He [10] and a fully microscopic description of its decay [11]. A study within

*Present address: Department of Physics, University of Richmond, Richmond, Virginia 23173, USA.
†Present address: University of Seville, E-41012 Sevilla, Spain.
‡Present address: ISOLDE, CERN, Geneva, Switzerland.
§Present address: Centre for Space Radiations (CSR), UCL, Louvain-la-Neuve, Belgium.
‖Present address: IPN, IN2P3/CNRS and Université Paris Sud, F-91406 Orsay Campus, France.
¶Present address: Department of Physics, University of York, York YO10 5DD, UK.

the R-matrix framework [12] reached the same conclusions by including a contribution to the β-decay matrix element coming from the external region, using an $\alpha + {}^2n$ wave function with a two-body asymptotic form for the ground state of ^{6}He. The latter description is analogous to a decay route proceeding first to the breakup of ^{6}He into $^4\mathrm{He} + {}^2n$, followed by the β decay of the dineutron into a deuteron, as already suggested by Borge *et al.* [5] as a possibility to reproduce the experimental data. All these studies point to the high sensitivity of the branching ratio to the external part of the ^{6}He wave function, thus confirming that the β decay is a precise probe of the halo structure.

A more recent study [13] has reexamined the decay process by employing $\alpha + n + n$ three-body wave functions in hyperspherical coordinates for ^{6}He [14] and a potential model for the $\alpha + d$ scattering states. While confirming the cancellation effect, the authors point out that the agreement with experimental data is very sensitive to the node structure of the initial and final states (i.e., to the ^{6}He wave function and the $\alpha + d$ states as determined by the $\alpha + d$ potential). Small modifications of the latter potential may significantly vary the deuteron-emission branching ratio, and this can be used to obtain a good agreement with the data (as done in Ref. [13]). Conversely, one can argue that a potential should be used that consistently reproduces the ^{6}Li ground-state binding energy and the $\alpha + d$ phase shifts (with a "fair" agreement being provided by the potential used in Ref. [13]), thus using the deuteron-emission branching ratio as a test of the ^{6}He wave function. More precise experimental data would make this test more stringent and would also put stronger constraints on the parameters of the calculations.

Here we report on new experimental results obtained using an implantation technique that allowed for a precise normalization. This is the first time that ^{6}He nuclei are directly implanted in a highly segmented silicon detector. The technique has been described in a previous publication [15], along with preliminary results for the ^{6}He decay. In the new experiments discussed herein, we measured the branching ratio of the $\alpha + d$ channel with a precision of 6%, which is a significant improvement over earlier results. The transition probability as a function of the energy of the emitted particles was also obtained with a low-energy threshold at 350 keV (deuteron energy), as was done in previous measurements.

II. EXPERIMENTAL DETAILS AND RESULTS

The measurements were done at the Cyclotron Research Centre at Louvain-la-Neuve (Belgium) [16]. The experimental technique (implantation of the radioactive nuclei in a silicon detector) requires a beam of ions at an energy sufficiently high to perform the implantation. A beam of ^{6}He ions at an energy $E = 7.9$ MeV was obtained using two coupled cyclotrons and the on-line isotope-separation method. The radioactive ^{6}He nuclei (half-life $T_{1/2} = 0.807$ s [17]) were produced through the $^7\mathrm{Li}(p,2p)^6\mathrm{He}$ reaction by impinging on a LiF target with a 200-μA, 30-MeV proton beam provided by the CYCLONE30 cyclotron. After diffusion out of the target and ionization in an electron cyclotron resonance (ECR) source, the nuclei were injected into the CYCLONE110 cyclotron and postaccelerated to the required energy. The second cyclotron was tuned to act as a powerful mass separator, eliminating isobaric impurities to levels better than 10^{-3} [18]. At the detection station, the beam was directly implanted in a thin double-sided silicon strip detector (DSSSD), 78 μm thick. The energy of the beam was chosen to stop the ions around the middle plane of the detector. According to calculations performed with SRIM [19], the implantation depth was 40 μm with a straggling (FWHM of the depth distribution) smaller than 2 μm. The intensity of the beam was maintained at the low value of about 6000 ions/s to minimize detector damage and the dead time of the acquisition system. To obtain a rather uniform distribution on the detector surface, the beam was defocused using quadrupole lenses positioned about 2 m upstream from the detector. The implantation was confined within the detector surface by a collimator, having a square hole the size of the detector, positioned about 10 cm from the detector surface.

The DSSSD had an active area of 16×16 mm^2, and each face was divided into 48 strips with the strips on the back face perpendicular to the ones on the front face. A total of 2304 pixels were defined by requiring only two signals in coincidence, one from each side of the detector ("multiplicity 1-1" events). The energy calibration of all channels was performed using standard α-particle calibration sources, correcting for the effect of the dead layer of the detector. At low energy, linearity was checked using a pulser. Many details and characteristics of the detection technique are described in Refs. [15] and [20], so we review here only those aspects that are most relevant for the present measurements.

The Q value of the $\alpha + d$ channel in the β decay of ^{6}He is 2.033 MeV. The energy is shared among the electron, the neutrino, and the two ions. Since the leptons carry almost no momentum, the ions are emitted almost back to back with energies inversely proportional to their masses. The range of 1-MeV deuterons in silicon is 12.2 μm and as a result the ions do not escape from the detector. More precisely, because the interstrip distance measures 35 μm, the combined energy of the emitted α particle and deuteron is collected within a single pixel. Conversely, β particles have a much larger mobility and deposit only a very small energy into a pixel. With an electronic detection threshold just above 100 keV, only about 1.6% of the total electrons emitted by multiplicity 1-1 events were detected. For very few events, the maximum detected energy for electrons attained 600 keV. Above this energy, only one β particle out of more than 10^7 emitted is detected, as shown in an analysis of the detector behavior [20] based on previous measurements and a simulation of the detector response [15,21].

A small fraction of the events generated by the implantation of the ^{6}He nuclei produced signals in the energy range of interest (0.5 to 2 MeV) owing to incomplete charge collection in the detector and to ions scattered along the beam line that still reach the detector. In our measurements, this fraction was around 10^{-4}, two orders of magnitude larger than the branching ratio for deuteron emission, so that the $\alpha + d$ decay events could not be identified in the overwhelming implantation background. For this reason, the ^{6}He beam was modulated in periods of 1 s beam-on and 2 s beam-off, and

only the $\alpha + d$ events occurring during the beam-off period were accepted. The beam modulation was achieved using a 1/3 Hz rotating shutter wheel with a 120° cutout placed in the beam path. The wheel also activated a photoresistor at each turn, giving a time reference that defined the beam-on and beam-off periods.

Instantaneous and complete suppression of the ion beam (to a level significantly better than 10^{-6}) required attention to various experimental factors. The use of a deflection magnet as described in Ref. [15] did not completely eliminate beam events during the beam-off period. With the use of a shutter wheel, the beam needs to be well collimated at the wheel position to avoid stray scattered particles from reaching the implantation detector. The precise definition of the transition between beam-on and beam-off periods is also important in calculating the number of decay events expected within a chosen time window. During our campaign we performed three measurements (including the one reported in Ref. [15]) on the ^{6}He nucleus to improve on these aspects of the experiment.

Figures 1(a) and 1(b) show the energy spectrum of all events recorded during the beam-off periods in Runs 2 and 3, respectively (the same spectrum for Run 1 is presented in Fig. 8 of Ref. [15]). For Run 3, the dynamics of such events is shown in the inset of Fig. 1(b). The exponential fit gives a half-life $T_{1/2} = 801(10)$ ms, as expected from the decay of ^{6}He. The uncertainty is mainly due to dead-time corrections that distort the decay curve. In the energy spectrum, pure β-decay events induce signals that decrease exponentially in number to a maximum energy of about 600 keV. The events at higher energy are due to the $\alpha + d$ emission channel (up to 2 MeV) plus any background. The presence of the latter is evident for Run 2 where events up to 6 MeV and beyond appear in the spectrum [see inset of Fig. 1(a)].

The background has two possible sources: I. constant background due to residual decay activity present in the detection chamber or due to cosmic rays and II. beam particles leaking through to the detector, around the shutter wheel, during beam-off periods (with a small fraction of them being capable of generating a signal in the energy range of interest). Type I events were evaluated in long, repeated off-line background measurements, with the detection chamber in the same location and conditions as during the actual beam irradiation. An observed weak α-decay activity was caused by a mechanical component in the detector chamber that had been contaminated by the calibration sources. The event rate was found to be essentially constant over the various runs and amounted to 1.2 ± 0.1 events/h, of which only 0.10 ± 0.02 events/h were in the energy range of interest. Given the total irradiation time in each run (10–80 h), one can see that this contribution is small. Type II events are revealed by the presence of events at full implantation energy during the beam-off period. This was observed during Runs 1 and 2, but completely suppressed in Run 3 by improvements in the shutter wheel system. Using this improved setup we later measured in Run 4 the decay of the pure β^+ emitter ^{18}Ne ($T_{1/2} = 1.67$ s [22], $Q_{\beta^+} = 3.424$ MeV, which is similar to that of ^{6}He). As discussed in Ref. [20], no events were observed in the energy range 0.6–2.0 MeV for 1.30×10^8 implantations, placing an upper limit of 4 events on the corresponding range

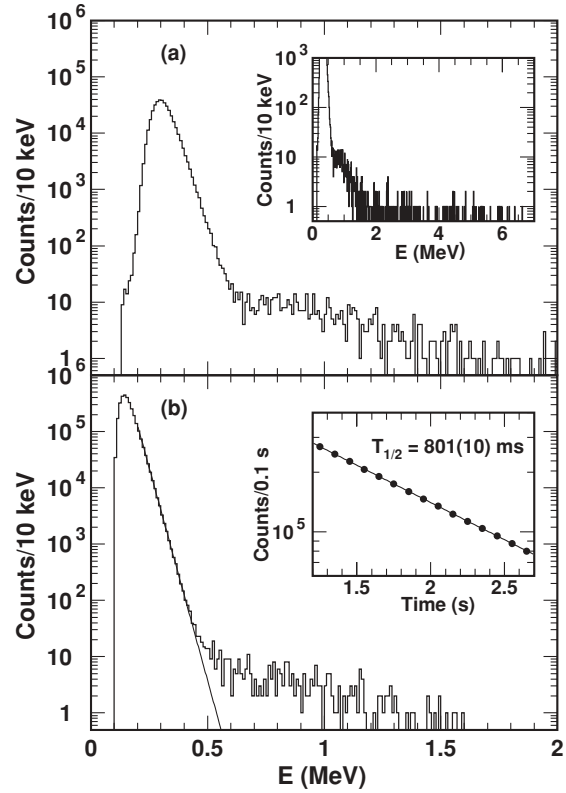

FIG. 1. (a) Total-energy spectrum of events detected during the beam-off period following the implantation of ^{6}He in Run 2. The inset of (a) shows the same spectrum up to 7 MeV. Panel (b) presents the results of Run 3, which were done under the same conditions as Run 2. The β-particle signals have a maximum energy of about 600 keV. Above this value, events are due to $\alpha + d$ emission events. The thin solid line in (b) is an exponential function fitted to the β-particle spectrum up to 400 keV. The inset of (b) shows the time behavior of all decay events, where the time scale refers to the beginning of the beam-on period.

in Run 3 (where the observation time was four times longer). For the previous runs, type II background was estimated from the number of detected implantations in the beam-off period and the fraction, 10^{-4} [15], that would induce the background. Also, an analysis was made of the dynamics of the events of interest (between 0.6 and 2.0 MeV), as shown in Fig. 2. When only decay events were present (as in Run 3, Fig. 2 top), an exponential fit gave a half-life $T_{1/2} = 0.83(18)$ s as expected for ^{6}He. For Run 2 (Fig. 2 bottom), a fit to a pure exponential decay gave a slower decay rate [where the corresponding half-life would have been $T_{1/2} = 1.10(17)$ s], indicating the presence of a constant background. A second fit, this time using an exponential function fixed at the known ^{6}He decay rate plus a constant offset (free parameter), provided a quantitative estimate of the background.

Table I summarizes the relevant quantities for each run. The "events above β's" are those between 0.525 and 2 MeV detected during the beam-off period (with the "observation window" indicating the fraction of observed decays). Where necessary, β events were subtracted using an exponential fit (see Fig. 1). The net $\alpha + d$ events are obtained by taking

TABLE I. Summary of the measurements with the ^{6}He and ^{18}Ne beams. See text for the definition of the $\alpha + d$ events. The weighted mean of the results for the branching ratio of ^{6}He into $\alpha + d$ is $\bar{B} = (1.65 \pm 0.10) \times 10^{-6}$.

Run	Duration	Implanted ions	Observation window	Events above β's	Background events	Net $\alpha + d$ events	Dead-time beam off	Branching ratio (in 10^{-6})
1 (^{6}He)	10^h20^m	1.86×10^8	32%	96 ± 20	1 ± 1	95 ± 20	5.0%	1.7 ± 0.4
2 (^{6}He)	73^h05^m	5.11×10^8	42%	587 ± 24	162 ± 69	425 ± 73	4.0%	2.0 ± 0.4
3 (^{6}He)	82^h30^m	4.61×10^8	44%	319 ± 18	4 ± 4	315 ± 18	4.2%	1.62 ± 0.11
4 (^{18}Ne)	25^h47^m	1.30×10^8	29%	–	–	–	–	–

into account the background sources of type I and II just described (together in Table I). The branching ratio of the deuteron-emission channel is then calculated by dividing the number of $\alpha + d$ events by the number of implanted ions, and corrections are applied for the time window of the observation and for the dead time of the acquisition system. Besides the error on the number of $\alpha + d$ events, the main additional uncertainty comes from the count of the implanted ions, for which a fraction induces signals on two adjacent strips when the implantation occurs close to their common edge. This effect depends on the beam energy and for ^{6}He contributes to 5% of the total error. The weighted mean of the branching ratio values measured in the three runs is $\bar{B} = (1.65 \pm 0.10) \times 10^{-6}$. The energy threshold above which events were counted was $E_{\text{c.m.}} = 525$ keV, corresponding to a deuteron energy $E_d = 350$ keV. This threshold is the same as the values reported in Refs. [4–6].

Since the energy dependence of the background present in Runs 1 and 2 was not known, a reliable energy spectrum of the $\alpha + d$ events was obtained using only the data collected in Run 3. A procedure was adopted to subtract the β events at low energy, by fitting them with an exponential function as shown in Fig. 1(b). The resulting $\alpha + d$ spectrum is shown in Fig. 3 in units for the transition probability, together with the data from Ref. [6] and the theoretical prediction from Ref. [13].

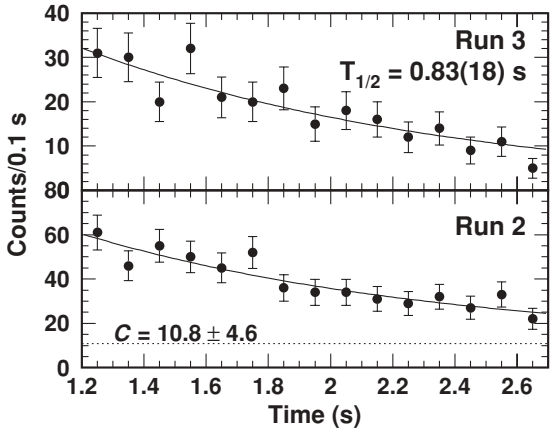

FIG. 2. Dynamics for events with an energy between 0.6 and 2 MeV detected in the beam-off periods after the implantation of ^{6}He. The top panel shows Run 3, the bottom panel shows Run 2, and the time scale refers to the beginning of the beam-on period. Events in Run 3 were fitted with a single exponential (solid line) that yielded a half-life $T_{1/2} = 0.83(18)$ s. For Run 2, the solid line is a two-component fit, with a constant offset (free parameter C) plus an exponential function with the decay rate of ^{6}He. The dotted line shows the level of the fitted offset. The result indicates that, of the total 587 ± 24 events, 162 ± 69 are due to background.

III. DISCUSSION

The energy spectrum of the $\alpha + d$ events measured using our technique agrees very well with the data from Ref. [6], both in shape and magnitude. We confirm the low value of the branching ratio for this channel and considerably reduce its uncertainty, from 50% to 6%. The new value corresponds to a transition probability $W = (1.42 \pm 0.09) \times 10^{-6}$ s^{-1} (for a deuteron energy $E_d \geqslant 350$ keV). The low value is due to the cancellation between two parts of the Gamow-Teller matrix element, as pointed out in Ref. [9] and then confirmed by several successive theoretical calculations. The various models [8,11–13], briefly reviewed in Sec. I, agree in predicting ratios on the order of 10^{-6}. We base our discussion on these calculations because they cover the approaches presently viable. With the improved precision of our results, a more thorough comparison becomes possible.

The Gamow-Teller matrix element connects the initial ^{6}He ground-state and final scattering $\alpha + d$ wave functions through the well-known spin-isospin operators. The cancellation takes place between the contributions of two separate regions of the

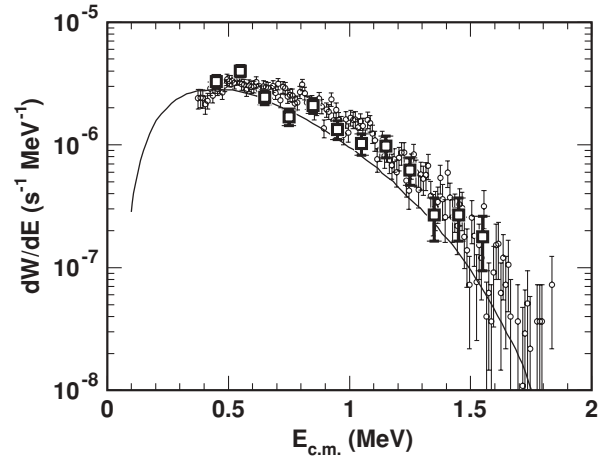

FIG. 3. Transition probability as function of the center-of-mass energy $E_{\text{c.m.}}$ for the $\alpha + d$ branch of the β decay of ^{6}He. The squares are our results from Run 3 and circles are data from Ref. [6]. The solid line is the prediction from Ref. [13] corresponding to a Gaussian $\alpha + d$ interaction potential (V_m in Ref. [13]).

spatial integral; the exact amount depends upon the choice of *both* the ^{6}He and $\alpha + d$ wave functions. It is therefore difficult to separately draw conclusions about the two. However, from the analysis of Refs. [11] and [13], some points clearly emerge. Consider first the $\alpha + d$ wave function. The correct order of magnitude of the branching ratio is reproduced only if such a wave function has two nodes, one of which is located at small distances. If the wave function is calculated from a potential model as in Refs. [8] and [13], the result depends upon the choice of the $\alpha + d$ potential. In Fig. 3 we show the transition probability from Ref. [13], corresponding to a Gaussian potential (the one shown is the V_m appearing in the Erratum [13]) capable of reproducing at the same time the experimental ^{6}Li binding energy and (fairly) the $\alpha + d$ low-energy phase shifts. The authors show that a better agreement can be achieved by a small renormalization of the potential. In Ref. [8] the $\alpha + d$ wave function does not have nodes, which is one of the reasons for the large overestimate (by about a factor 20) of the branching ratio. In the parameter-free model of Ref. [11] the agreement is again good (the prediction being about a factor of 2 larger than our measured value). The $\alpha + d$ wave function is there obtained from a microscopic calculation employing a nucleon-nucleon potential; the choice of the basis states makes it possible, both here and in Ref. [13], to reproduce both the ^{6}Li binding energy and $\alpha + d$ phase shifts. This discussion does not apply to the R-matrix calculation of Ref. [12], because in this case an overall normalization can be absorbed in the fitted constants, reaching the correct order of magnitude for the branching ratio. With this approach, only the asymptotic form of the $\alpha + d$ wave function (thus the phase shifts) enters the calculation.

Precise agreement with the experimental data also requires the correct form of the ^{6}He ground-state wave function. Because the level of the cancellation in B_{GT} is very large, small contributions are important. The wave function should be correctly described up to large distances—in Ref. [13], it was required to extend the spatial integral up to 30 fm to achieve convergence. For the same reason, the wave function needs to be "complete," including also weak components. Depending on the description employed, this completion can be achieved by the choice of a sufficiently large configuration basis (as for the microscopic model in Ref. [11]) or by the inclusion of the components with a large hypermomentum (as for the hyperspherical-coordinates model of Ref. [13]). Besides the value of the overall branching ratio, the energy dependence of the transition probability (Fig. 3) constitutes a further constraint. As shown in Ref. [13], the use of a two-body asymptotic form for the ^{6}He wave function (as in Ref. [12] for example), instead of a three-body one, can cause a distortion of the spectrum on the order of 30% (this being the difference in the ratios of the values of dW/dE at 0.5 and 1.0 MeV between the two models). The present experimental results confirm the need of using a ^{6}He ground-state wave function having the correct three-body asymptotic behavior. The position of the maximum of the experimental data and of the theoretical prediction still differ slightly, but a small modification of the potential can lead to a better agreement [13]. However, it would also be desirable to extend the measurement down to lower energies to reduce uncertainties.

The transition probability is very sensitive to the precise location of the nodes in the wave functions (and, for the $\alpha + d$ wave function, to their behavior at different scattering energies). The present measurement can be used as a stringent test of the ^{6}He (halo) wave function only if a consistent description is adopted for all the states involved. In Ref. [13] an accurate wave function in hyperspherical coordinates is used for ^{6}He, but obtaining the $\alpha + d$ scattering wave function from a potential model allows for a degree of freedom (the potential) that can be used, within certain limits, to fit the transition probability independently from the description of ^{6}He. (We stress again that, in principle, the potential could be fixed by requiring a better fit of the $\alpha + d$ phase shifts.) So far, the only fully consistent approach is the parameter-free, microscopic calculation of Ref. [11]. Within this model, both the ^{6}He and ^{6}Li binding energies are reproduced, as well as the $\alpha + d$ phase shifts. However, the total branching ratio is overestimated by a factor of 2 and the shape of the transition probability as a function of the energy is different, being similar in magnitude to the experimental data at 1.5 MeV but about a factor of 3 larger at 0.5 MeV. Improvements can be sought by changing the basis functions, for example by enlarging the range of the intercluster distances in the various configurations (with 20 fm being the range used in Ref. [11]).

IV. CONCLUSIONS

We measured the weak $\alpha + d$ branch in the β decay of the halo nucleus ^{6}He by implanting ^{6}He postaccelerated ions into a silicon detector and observing the signal from the emitted particles. The weighted mean of three successive measurements gave a branching ratio $\bar{B} = (1.65 \pm 0.10) \times 10^{-6}$, corresponding to a transition probability $W = (1.42 \pm 0.09) \times 10^{-6}$ s^{-1} for a deuteron energy $E_d \geqslant 350$ keV. The sum energy spectrum of the emitted ions was also measured. Our results are in agreement with the most recent experimental results from Ref. [6] and are about a factor of 5 smaller than those reported in Ref. [5]. The precision of the branching ratio is significantly improved in the present measurement. Existing calculations [9–11,13] show that the quenching of the branching ratio is due to a cancellation in the Gamow-Teller matrix element between contributions from different parts of the spatial integral. To achieve such a large quenching and reproduce the correct energy dependence of the transition probability dW/dE, precise requirements are placed on the initial ^{6}He and final $\alpha + d$ wave functions. In particular, the former needs to be specified up to very large distances (about 30 fm) and to possess the correct three-body asymptotic form. To reduce the uncertainties in the models, future measurements should aim at extending the $\alpha + d$ spectrum to even lower energies.

ACKNOWLEDGMENTS

We thank L. Buchmann and P. Descouvemont for providing the data from Refs. [6] and [13], respectively, in tabular form. R.R. acknowledges postdoctoral research support from the

Fund for Scientific Research-Flanders (Belgium) (F.W.O.–Vlaanderen). This work was supported by the Interuniversity Attraction Poles Programme–Belgian Science Policy (IUAP) under Project P5/07.

[1] P. G. Hansen, A. S. Jensen, and B. Jonson, Annu. Rev. Nucl. Part. Sci. **45**, 591 (1995).
[2] M. J. G. Borge *et al.*, Z. Phys. A **340**, 255 (1991).
[3] I. Mukha *et al.*, Phys. Lett. **B367**, 65 (1996).
[4] K. Riisager *et al.*, Phys. Lett. **B235**, 30 (1990).
[5] M. J. G. Borge, L. Johannsen, B. Jonson, T. Nilsson, G. Nyman, K. Riisager, O. Tengblad, and K. Wilhelmsen Rolander (ISOLDE Collaboration), Nucl. Phys. **A560**, 664 (1993).
[6] D. Anthony, L. Buchmann, P. Bergbusch, J. M. D'Auria, M. Dombsky, U. Giesen, K. P. Jackson, J. D. King, J. Powell, and F. C. Barker, Phys. Rev. C **65**, 034310 (2002).
[7] P. Descouvemont and C. Leclercq-Willain, J. Phys. G **18**, L99 (1992).
[8] M. V. Zhukov, B. V. Danilin, L. V. Grigorenko, and N. B. Shul'gina, Phys. Rev. C **47**, 2937 (1993).
[9] D. Baye, Y. Suzuki, and P. Descouvemont, Prog. Theor. Phys. **91**, 271 (1994).
[10] K. Varga, Y. Suzuki, and Y. Ohbayasi, Phys. Rev. C **50**, 189 (1994).
[11] A. Csótó and D. Baye, Phys. Rev. C **49**, 818 (1994).
[12] F. C. Barker, Phys. Lett. **B322**, 17 (1994).
[13] E. M. Tursunov, D. Baye, and P. Descouvemont, Phys. Rev. C **73**, 014303 (2006); **74**, 069904(E) (2006).
[14] P. Descouvemont, C. Daniel, and D. Baye, Phys. Rev. C **67**, 044309 (2003).
[15] D. Smirnov *et al.*, Nucl. Instrum. Methods Phys. Res. A **547**, 480 (2005).
[16] G. Ryckewaert, J. M. Colson, M. Gaelens, M. Loiselet, and N. Postiau, Nucl. Phys. **A701**, 323c (2002).
[17] D. R. Tilley, C. M. Cheves, J. L. Godwin, G. M. Hale, H. M. Hofmann, J. H. Kelley, C. G. Sheu, and H. R. Weller, Nucl. Phys. **A708**, 3 (2002).
[18] D. Miljanic *et al.*, Nucl. Instrum. Methods Phys. Res. A **477**, 544 (2000).
[19] J. F. Ziegler, J. P. Biersack, and U. Littmark, *The Stopping and Range of Ions in Solids* (Pergamon Press, New York, 1985).
[20] J. Büscher, J. Ponsaers, R. Raabe, M. Huyse, P. Van Duppen, F. Aksouh, D. Smirnov, H. O. U. Fynbo, S. Hyldegaard, and C. A. Diget, Nucl. Instrum. Methods Phys. Res. B **266**, 4652 (2008).
[21] R. Raabe *et al.*, Phys. Rev. Lett. **101**, 212501 (2008).
[22] D. R. Tilley, H. R. Weller, C. M. Cheves, and R. M. Chasteler, Nucl. Phys. **A595**, 1 (1995).